Environmental Science and Pollution Research (2019) 26:37001–37011
https://doi.org/10.1007/s11356-019-06775-7

RESEARCH ARTICLE

Characteristics, speciation, and bioavailability of mercury and methylmercury impacted by an abandoned coal gangue in southwestern China

Longchao Liang[1,2] · Xiaohang Xu[2,3] · Jialiang Han[2] · Zhidong Xu[2,3] · Pan Wu[1,4] · Jianyang Guo[2] · Guangle Qiu[2]

Received: 28 May 2019 / Accepted: 15 October 2019 / Published online: 19 November 2019

Abstract

During coal mining activities, a lot of coal gangue is produced, which usually contains high mercury (Hg) concentrations as well as the acid mine drainage (AMD) generator of pyrite. In the present study, the total mercury (THg) and methylmercury (MeHg) in gangue, water, sediment, paddy soil, and rice samples, collected from abandoned coal mining areas, were analyzed. Results showed that the THg concentrations ranged from 0.37 to 35 mg/kg (11 ± 8.4 mg/kg) and 0.15 to 19 mg/kg (2.0 ± 3.9 mg/kg) in gangue and sediments, respectively. For paddy soils, the THg concentrations and MeHg varied from 0.16 to 0.91 mg/kg and 0.71 to 11 ng/g, respectively. Rice samples exhibited wide concentration ranges of THg (3.0–22 ng/g) and MeHg (0.71–8.9 ng/g). Sequential extraction of Hg revealed that the nitric acid-extractable state Hg (F4) was the dominant Hg species in gangue and sediment, while humic acids state Hg (F3) was the dominant form in paddy soil. Compared with gangue, higher percentages of F3 and the residual state Hg (F5) in both sediment and soil samples implied the transformation of F4 to F3 and F5 during transportation. Soil n-HAs (the difference between the total organic carbon and humic acids) were positively correlated with both THg and MeHg in soil and rice, indicating that n-HAs enhance Hg bioavailability under acidic conditions. Further studies should be conducted to reveal the factors influencing the transformation of different Hg fractions, providing ideas on decreasing the bioavailability of Hg in coal mining areas.

Keywords Total mercury · Methylmercury · Mercury speciation · Biogeochemsitry · Influencing factors · Coal mining activities

Introduction

Mercury (Hg) is a highly toxic heavy metal that occurs in different forms in the environment, including elemental Hg (Hg^0), inorganic Hg, and organic Hg. Since Hg^0 that is emitted into the air is able to travel long distances in the atmosphere, it is considered to be a global pollutant (Lindberg and Stratton 1998). The airborne Hg circulating in the atmosphere eventually deposits back onto the Earth's surface in rainfall or in the dry gaseous form (Korosi et al. 2018). Once deposited, Hg can go through a series of chemical transformations to methylmercury (MeHg), a highly toxic organic form that is readily accumulated and biomagnified in food chains (Hintelmann et al. 2002). Although only a minute fraction of Hg is present as MeHg in the environment, it is of the highest concern due to its biomagnification in the food web (Lee and Fisher 2017).

Both natural and anthropogenic emissions contribute to the global Hg reservoir, and the latter mainly includes artisanal and small-scale gold mining, coal combustion, non-ferrous metal production, cement production, and Hg-added product

Responsible editor: Severine Le Faucheur

Electronic supplementary material The online version of this article (https://doi.org/10.1007/s11356-019-06775-7) contains supplementary material, which is available to authorized users.

✉ Pan Wu
pwu@gzu.edu.cn

[1] College of Resource and Environmental Engineering, Guizhou University, Guiyang 550025, China

[2] State Key Laboratory of Environmental Geochemistry, Institute of Geochemistry, Chinese Academy of Sciences, Guiyang 550081, China

[3] University of Chinese Academy of Sciences, Beijing 100049, China

[4] Key laboratory of Karst Environment and Geohazard, Ministry of Land and Resources, Guiyang 550025, China

usage (Wu et al. 2018). Among the anthropogenic emission sources, approximately 21% of Hg emissions were attributing to stationary coal combustion, the second largest contributor after artisanal gold mining. And the estimated global emissions of Hg into the atmosphere from anthropogenic sources in 2015 were approximately 20% higher than they were in 2010 (UNEP 2018). China highly depends on coal energy, and coal combustion contributed nearly 50% of the Hg emissions in China (Wang et al. 2012; AMAP/UNEP 2013; Tian et al. 2013; BP 2015; Zhang et al. 2015). These emissions cause concern regarding their impact on the health of wildlife and human populations.

Better knowledge of the Hg concentrations in the coals of China has been achieved. The results for the average concentrations of Hg in Chinese coals ranged from 0.15 to 0.20 μg/g (Ren et al. 2006; Bai et al. 2007; Dai et al. 2012; Tian et al. 2013), which were higher than that of 0.10 μg/g in world coals (Ketris and Yudovich 2009). The coal-bearing regions in southwestern China are enriched in Hg. As high as 22.5 μg/g Hg was reported in the coal from the Guizhou Province (Zhang et al. 2002). Those elevated Hg in coals could result in significant Hg emissions with high atmospheric Hg deposition occurring in areas inside and downwind of the stationary combustion sources, eventually causing risks to the ecosystems and human health (Xu et al. 2017a). Recent studies revealed the impact of atmospheric Hg deposition on the surroundings of coal-fired power plants (Xu et al. 2017a; Li et al. 2017) and found that approximately 79% of vegetables and 67% grain samples exceeded the PTWI's food safety standards of maximum Hg concentrations of 10 ng/g in vegetables and 20 ng/g in grains (GB 2762-2012). They also found that rice grain tended to have high MeHg concentrations.

In coal mining areas, gangue is the dominant coal mining waste. Considering the highest coal production in China, coal gangue is estimated to reach 4.5–5 Gt with an annual increase of 0.37–0.55 Gt (Liang et al. 2016). Due to its low heating value, significant quantities of gangue were stored in open-air adjacent to coal mining sites. Notably, gangue has a higher concentration of Hg than coal (Zhai et al. 2015).

Recently, researchers have conducted several studies on Hg released from gangue during the heating process, indicating that gangue may be an important contributing factor to the anthropogenic Hg inventory (Zhai et al. 2015; Liang et al. 2014, 2016; Zhao et al. 2017; Wu et al. 2019). Furthermore, gangue also releases inorganic Hg into aquatic systems (Liang et al. 2018). Long-term weathering and AMD may enhance the leakage and release of Hg due to the low pH. Hence, the legacy Hg in gangue may act as a major source of inorganic Hg to the surroundings, which can be bio-transformed into MeHg and accumulate in the local crops. However, how AMD influence the speciation and bioavailability of Hg and MeHg in coal mining areas are still poorly understood. Hence, a better understanding of the levels of Hg contamination, particularly MeHg, in the environment impacted by the coal mining activity is necessary.

To address the knowledge gap, we measured the concentrations of THg and MeHg in gangue, water, sediment, soil, and rice from abandoned coal mining areas to evaluate Hg contamination, distribution, and their influential factors under acidic condition. The sequential extraction of Hg chemical forms in gangue, sediment, and soil were investigated to elucidate their mobilization mechanism.

Materials and methods

Study area

The Jiaole coal mine (25° 09′ N, 105° 21′ E) is located 20 km southwest of Xingren City in the Guizhou Province in southwestern China, and it covers approximately 15 km^2 (Fig. 1). The region is hilly and karstic with an elevation of 1785 m. The climate is characterized as a mild and humid subtropical monsoon climate. The average annual temperature is 15 °C, and the average annual rainfall is 1400 mm. The prevailing wind direction is from the southwest throughout the entire year. The coal-bearing strata are mainly in the Permian Longtan Formation. Mudstones, silt-mudstones, and siltstones generally present at the top of the coal layers, which are composed of clay rock and sandstone mixed with coal and limestone, flinty carbonate, and siliceous shale, respectively (Wu et al. 2009). The Lugou River flows through the Jiaole mining district and has been directly impacted by the historic coal mining activity. Two tributaries, the Maoshitou and Shitouzhai streams, flow across the coal mining district and finally flow into the Lugou River at a confluence in the Jiaole Village.

The coal mining activity in Jiaole experienced approximately 40 years and closed in the early 2000s. The coal gangue covers a total area of 1.5 km^2 (1.5 km length, 0.5–1.5 km width). The dominant ore mineral of Jiaole is anthracite, characterized by high levels of Au, As, Hg, and F (Li and Wu. 2017). Huge gangue piles and waste rocks combined with gangue can be observed. Most of the coal mine solid wastes were piled along the Maoshitou and Shitouzhai streams without any treatment. The drainage and runoff through the gangue piles directly flows into tributaries of the Lugou River. Approximately 3200 people of the Jiaole Village live downstream, whose staple food is rice locally yielded from paddies irrigated by acid mine drainage.

Sampling and sample preparation

Sampling campaign was conducted at a total of 42 sites (28 along with mainstream, 14 along the tributaries) in the Jiaole coal mining area during the rice harvest season in September 2017. Coal gangue samples ($n = 39$) were randomly collected

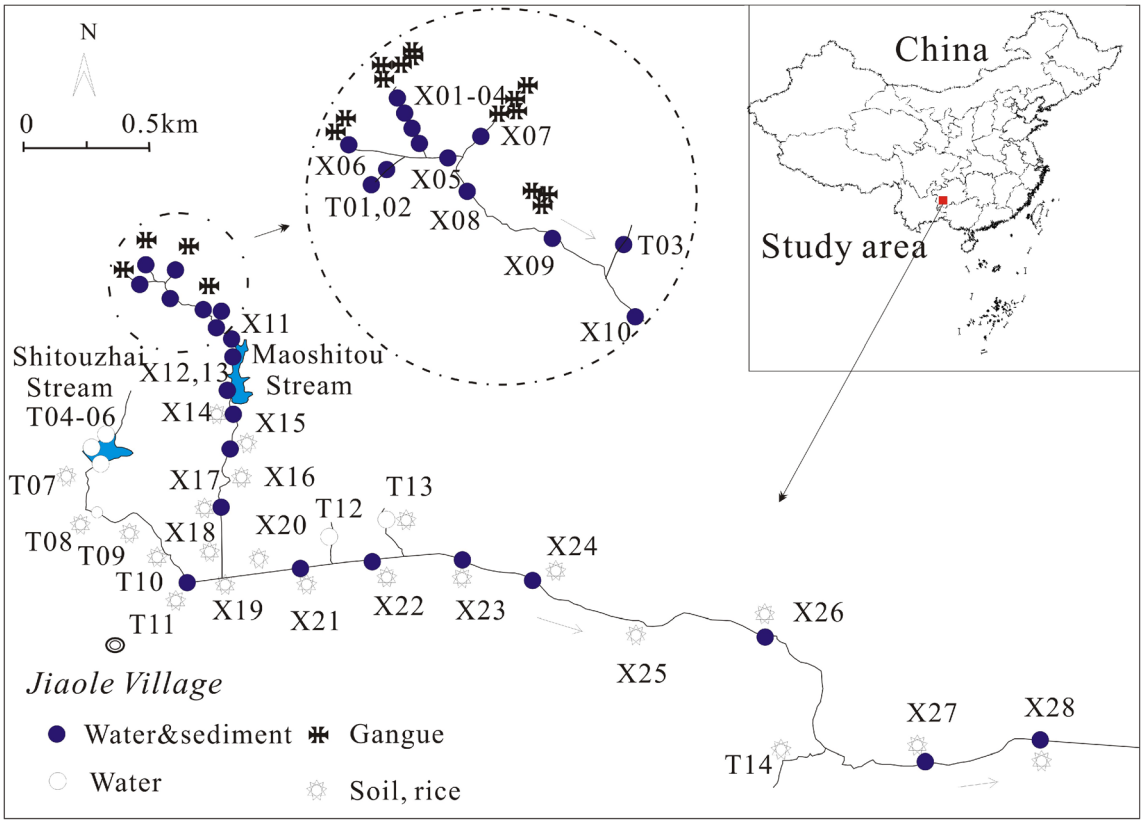

Fig. 1 Study area and sampling sites

from 5 to 20 cm from gangue piles, and at each sampling site, the final sample was composed of 3–5 subsamples collected within an area of 25 m^2. Sediment ($n = 48$) and surface water samples ($n = 33$) were collected from the Lugou River as well as its tributaries. Approximately 100 mL of unfiltered surface water was collected in a 100-mL borosilicate glass bottle pre-cleaned by heating at 550 °C for 1.5 h. Sediment samples were collected from the surface layer (0–10 cm) and composited from 2 to 3 localities at each site within a 10-m distance along the river. Paddy soil samples ($n = 92$) were collected from farmlands irrigated by the nearby river. The soil samples were collected using a stainless-steel grab sampler and a plastic scoop, and each sample was a composite of 3 to 5 subsamples, for a total sample size of 0.5–1 kg. Simultaneously, rice grain samples ($n = 22$) and their corresponding soil samples were collected. Each rice sample was comprised of at least five subsamples within an area of approximately 25 m^2 in the same paddy field. Sampling information and sample numbers for each site are listed in Table S1 in the Supporting Materials.

After collection, all solid samples were stored in polyethylene bags to avoid cross-contamination. In the laboratory, the soil and sediment samples were air-dried, crushed, and passed through a 200-mesh sieve for subsequent analysis. For rice, the polished rice was separated using a mortar and pestle and ground to 200 mesh (IKA-A11 basic, Germany). Surface water samples for THg analysis were acidified with ultra-pure HNO_3 and for MeHg analysis; they were acidified with ultra-pure HCl to a final acid concentration of 0.4% (*v*/v) within 24 h of the collection (Qiu et al. 2012a). All water samples were stored in refrigerator (+ 4 °C) and the THg and MeHg in samples were measured within 28 days after collection.

Analytical methods

Gangue, sediment, and soil

Total Hg For the THg concentrations in gangue, soil and sediment samples, approximately 0.1–0.3 g of sample, were weighed and placed into a tube with a fresh mixed solution of HCl and HNO_3 (3:1, v/v), followed by heating to 95 °C for 30 min using a water bath. Then, BrCl was added, and the mixture was heated to 95 °C for another 30 min (Xu et al. 2017b). Afterwards, an appropriate amount of the digested solution was determined by cold-vapor atomic absorption spectrometry (CV-AAS, Brooks Rand).

MeHg For soil and sediment MeHg determination, approximately 0.2–0.5 g of dry sample was extracted with CH_2Cl_2 after leaching with a saturated solution of $CuSO_4$ and HNO_3 (Liang et al. 1996). Then, an appropriate amount of the digested solution was analyzed by GC-CVAFS according to US EPA Method 1630 (USEPA 2001).

Hg fractions A modified sequential extraction procedure (Bloom et al. 2003) was applied to analyze the Hg species in all of the solid samples. The water-soluble state Hg (F1), fulvic acid state Hg (F2), humic acid state Hg (F3), nitric acid-extractable state Hg (F4), and residual state Hg (F5) fractions were obtained via the extraction process. In brief, approximately 1.0 g of a solid sample was weighed and placed into a 50-mL centrifuge tube, and then, 45 mL of the extraction regent was added for each extraction step. The tube was then shaken for 24 h at room temperature. After that, the solution and the solid phase were separated by centrifugation at 3500 rpm for 20 min. The supernatant was removed and preserved in borosilicate glass for Hg analysis. The detailed extraction procedure is described in Table S2 in the Supporting Materials. The Hg was determined by cold-vapor atomic fluorescence spectroscopy (CVAFS) according to Method 1631E (USEPA 2002).

X-ray diffractometry The minerals in solid samples were identified via XRD analysis. The XRD data were collected on a PANalytical multifunction X-ray diffractometer (Empyrean, Malvern PANalytical Ltd., United Kingdom) equipped with an Anton Paar high-temperature accessory (APHTK-16N) and a 3D PIXcel detector. The XRD measurements were performed in a 2θ range of 4.1–60° in continuous scanning mode with a 0.026° step size and a counting time of 35 s per step.

TOC and pH in the soil and sediment The potassium dichromate oxidation spectrophotometric method was used to measure the total organic carbon (TOC) contents of the soil and sediment samples. The determination of humic acid, and fulvic acid were performed according to the method reported previously (NY-T-1867-2010) (Wang et al. 2019). The soil and sediment pH were measured by transferring 5 g of sample into 12.5 mL of deionized water and then analyzing the pH using a pH meter (LeiciZD-2; Shanghai, China).

Surface water

THg concentrations in water were measured after BrCl oxidation and $SnCl_2$ reduction by CVAFS detection according to Method 1631E (USEPA 1999). For MeHg, water samples were distilled, followed by NaBEt4 ethylation, Tenax trapping, and GC-CVAFS detection according to Method 1630 (USEPA 2001). The method requires a sequence of distillation, Tenax trapping, thermal desorption, GC separation, and CVAFS detection (Brooks Rand Model III, Seattle, USA).

Rice

For rice THg concentration measurements, approximately 0.5–1.0 g of rice sample was weighed and placed into a glass tube. Then, 5 mL of ultra-pure HNO_3 was added, and the sample was digested at 95 °C in a water bath for 3 h. After that, a suitable aliquot was measured using CVAFS. For measurement of the rice MeHg concentration, approximately 0.2–0.5 g of rice sample was digested using 25% KOH at 80 °C for 3 h. Then, MeHg in the rice sample was leached with CH_2Cl_2 and back-extracted into the water for determination according to Method 1630 (USEPA 2001).

QA/QC

The QA and QC of the THg and MeHg analyses were assessed using duplicates, method blanks, matrix spiking, and reference materials (GBW07405; BCR580, TORT-2). For gangue and soil samples, the THg in the certified reference material GBW07405 was measured, and the average concentration of 0.30 ± 0.06 ($n = 5$) observed was comparable with the certified value of 0.29 ± 0.04 μg/g. For sediment, THg in the certified reference material GBW07305a was measured and the average concentration of 0.30 ± 0.07 μg/g ($n = 5$) observed was comparable with the certified value of 0.29 ± 0.03 μg/g. The relative percentage difference of all measured values was less than 5%. For Hg species in all solid samples, the extraction efficiency was evaluated by calculating the ratio between the total amount of Hg in the extracted species and the THg concentration directly measured for the corresponding sample. The recoveries varied from 81 to 96% for gangue samples, from 92 to 118% for soil samples, and from 90 to 117% for sediment samples. For MeHg in sediment and soil samples, the BCR 580 was measured, and the obtained average concentration of 77 ± 8.0 ng g^{-1} ($n = 5$) confirmed the certified value of 75 ± 4.0 ng g^{-1}. The relative percent difference was less than 10%.

For water samples, the recoveries of matrix spike varied from 94 to 101% for THg and 88 to 109% for MeHg. The detection limits of THg and MeHg were 0.05 ng/L and 0.007 ng/L, respectively. The relative percentage differences were less than 10% for THg and less than 9% for MeHg in duplicates.

For rice samples, the TORT-2 reference material was used for MeHg determination, and the MeHg value of 150.9 ± 10.8 ng/g ($n = 5$) obtained was comparable with the certified concentration of 152 ± 13 ng/g. Matrix spike recoveries of THg and MeHg were 97–106% and 101–107%, respectively. The relative percentage differences were < 10% for THg and 6% for MeHg in duplicates. The detection limits for Hg and MeHg were 0.01 ng/g and 0.002 ng/g, respectively.

Results and discussion

THg and MeHg in gangue, sediment, and soil

Gangue samples exhibited highly varied THg concentrations, ranging from 0.37 to 35 mg/kg with an average of 11 ±

8.4 mg/kg. The total Hg in the sediment samples ranged from 0.15 to 4.4 mg/kg with an average of 1.3 ± 1.3 mg/kg, with the exception of sample X02, which contained a concentration as high as 19 mg/kg (Table S3 in the Supporting Materials). In contrast, paddy soils contained slightly low THg concentrations of 0.16–0.91 mg/kg with an average of 0.40 ± 0.22 mg/kg (Table 1). Generally, along the water flow, THg concentrations presented the order of gangue > sediment > soil. The concentrations of THg in the gangue samples in the present study were much higher than that in gangue samples from the Shanxi Province (Querol et al. 2008; Zhao et al. 2008), Shandong Province (Hua et al. 2018), Anhui Province (Cui et al. 2004; Cai et al. 2008), and Inner Mongolia Province (Liang et al. 2016). The high levels of Hg in gangue were well consistent with the elevated Hg reported in Xingren coal (Dai et al. 2006). This is probably due to its high geological background of Hg within the world largest circ-Pacific mercuriferrous belt (Qiu et al. 2005), and the elevated levels of Hg in gangue cause it to be a significant Hg source to the environmental surroundings.

Sediments collected from sites that were heavily impacted by gangue and its drainage, such as X01-X06, X09-X11, and X13, as expected, contained high Hg concentrations of greater than 1.1 mg/kg, indicating the riparian gangue Hg source. The high Hg concentrations in sediment samples generally decreased with increasing distance away from the gangue piles (Fig. S1). Similarly, paddy soils collected from upstream sites adjacent to gangue piles contained higher THg concentrations than those from downstream sites, suggesting that Hg-enriched particles are transported from the upstream Hg source of gangue and/or re-suspended sediment during flooding and/or irrigation. Compared with the probable effect Hg concentration (PEC) of 1.06 mg/kg (MacDonald et al. 2000), the sediments (> 1.1 mg/kg) could become a threat to dwelling organisms, which constitute the main reservoir of Hg in the aquatic ecosystem in the Xingren mining area.

Both sediment and soil samples exhibited a wide range of MeHg concentrations, varying from 0.036 to 7.8 ng/g and from 0.71 to 11 ng/g, respectively. Peak concentrations of MeHg in sediments were found at sites proximal to gangue piles (X09, 7.8 ng/g) and at sites distances downstream (X20, 5.2 ng/g; X24, 5.3 ng/g). High percentages of MeHg to THg in paddy

Table 1 Concentrations of THg and MeHg in soil and rice, and other parameters in soil.

Sample ID	Soil							Rice	
	THg (mg/kg)	MeHg (ng/g)	TOC (%)	HA (%)	FA (%)	n-HA (%)	pH	THg (ng/g)	MeHg (ng/g)
X14	0.47	2.2	2.85	0.30	1.2	2.6	4.33	9.4	4.1
X15	0.56	3.2	3.73	0.93	1.2	2.8	4.78	6.0	3.5
X16	0.55	1.7	4.06	1.1	1.3	3.0	4.58	9.5	3.9
X17	0.86	2.8	3.85	1.3	0.74	2.6	5.09	12	4.9
X18	0.91	8.3	3.49	0.89	1.8	2.6	5.62	12	3.6
X19	0.63	11	3.84	0.86	0.97	3.0	5.70	18	8.9
X20	0.62	9.0	3.35	1.1	0.72	2.2	5.94	4.9	2.1
X21	0.61	6.6	3.52	1.0	0.96	2.5	6.09	15	7.8
X22	0.32	1.8	3.34	1.4	0.73	2.0	7.07	4.9	1.3
X23	0.23	1.3	2.82	1.5	0.68	1.3	6.82	5.9	2.5
X24	0.22	1.6	2.62	1.2	0.17	1.4	6.71	8.7	2.3
X25	0.25	1.5	2.65	1.7	0.70	0.95	6.32	7.0	0.96
X26	0.22	0.92	2.78	0.84	0.94	1.9	6.64	5.0	0.71
X27	0.22	1.3	3.01	0.83	0.61	2.2	6.78	3.9	0.94
X28	0.20	0.71	2.33	0.97	0.41	1.4	6.73	3.0	0.85
T07	0.18	3.0	3.31	0.54	1.3	2.8	6.19	7.0	2.2
T08	0.19	2.3	3.61	0.82	0.84	2.8	6.62	8.7	3.8
T09	0.21	3.8	3.28	0.60	1.3	2.7	6.96	22	8.2
T10	0.60	5.3	3.43	0.96	0.37	2.5	6.18	12	5.9
T11	0.41	1.3	2.56				6.23		
T12	0.32	2.9	3.91				5.21		
T13	0.31	1.6	3.21				7.03		
T14	0.16	1.4	2.27	0.72	0.99	1.5	6.92	3.1	1.4
Mean	0.40 ± 0.22	3.28 ± 2.83	2.27–4.06	0.30–1.7	0.17–1.8	0.95–3.0	4.33–7.07	8.9 ± 5.0	3.5 ± 2.5

soils were found and ranged from 0.31 to 1.8% with an average of 0.82 ± 0.47%, probably attributed to the in situ favorable conditions of the pH and organic matter for Hg methylation (Ullrich et al. 2001; Galloway and Branfireun 2004). The elevated MeHg concentrations as well as their high percentages could be eventually accumulated and biomagnified in the food web, posing a potential health exposure risk.

THg and MeHg in water and rice

Surface water samples contained a wide range of THg concentrations, ranging from 1.0 to 11 ng/L with an average of 3.8 ± 2.3 ng/L. MeHg concentrations varied widely as well, from 0.008 to 0.37 ng/L with an average of 0.11 ± 0.093 ng/L (Table S3). A conversion rate of THg to MeHg as high as 18% was observed in the water samples, suggesting an active Hg methylation process in the aquatic ecosystems of the region, which should be further investigated. Moreover, high concentration of SO_4^{2-} (1370 ± 314 mg/L) in Maoshitou Reservoir and downstream in Lugou River (419 ± 449 mg/L) were reported by our group (Zhang et al. 2013). The high SO_4^{2-} may be the key factor promoting the Hg^{2+} methylation by sulfate-reducing bacteria (Shipp and Zierenberg 2008). Considering the elevated concentrations of Hg in the sediment samples as well as the highest value of THg (X02) being observed at a site adjacent to the huge gangue piles, high levels of Hg in the gangue may be the primary Hg source to the local aquatic systems, which can be attributed to the continually accumulating input of Hg from the untreated tailings by weathering and/or leaching processes. A positive correlation ($r^2 = 0.380$, $p < 0.005$) was found between the sediment THg and water THg, suggesting that Hg-contaminated sediment might be the major source of Hg in the water, from which abundant Hg can be released into overlaying water under the acidic conditions.

Rice samples exhibited high concentrations of Hg, ranging from 3.0 to 22 ng/g with an average of 8.9 ± 5.0 ng/g for THg and from 0.71 to 8.9 ng/g with an average of 3.5 ± 2.5 ng/g for MeHg. High percentages of MeHg to THg were observed in samples, ranging from 14 to 58% with an average of 37 ± 12%. The highest value of 22 ng/g THg exceeded the Chinese national permitted limit of 20 ng/g Hg in cereals (NSA 1994). Compared with the data for samples from sites impacted by coal-fired power plants (Xu et al. 2017a) and that for rice observed at the control site (Meng et al. 2010), the concentrations of THg in rice of the Xingren coal mining area were high. Elevated THg and MeHg as well as high MeHg percentages observed in rice grains in the present study implied that Hg released from coal mining can be readily biomethylated into MeHg, which can be accumulated in rice plants (Qiu et al. 2008). This phenomenon indicates that the coal mining areas with AMD are Hg-sensitive ecosystems.

Mercury speciation in gangue, sediment, and soil as well as their transforming potential

Five sequential extractions of Hg fractions in gangue, sediment, and soil samples indicate that the dominant forms of Hg were F4 and F3, accounting for 14.7–82.5% and 10.1–68.2% of the THg, respectively (Fig. 2). For gangue, different Hg fractions followed the order: F4 (82.5%) > F3 (10.1%) > F5 (5.46%) > F2 (1.6%) > F1 (0.37%). Similar to gangue, Hg fractions of sediments also had the flowing trend: F4 (49.2%) > F3 (25.7%) > F5 (21.7%) > F2 (3.44%) > F1 (0.057%). However, for paddy soils, Hg fractions followed a quite different order: F3 (68.2%) > F4 (14.7%) > F2 (8.55%) > F5 (8.15%) > F1 (0.36%). Along the water flow, from gangue via sediment to soil, F4 showed a decreasing trend from 82.5 to 14.7%. However, F3 exhibited an increasing trend from 10.1 to 68.2%. Although there were low percentages of F2 in gangue, sediment, and soil, an increasing trend (from 1.6 to 8.55%) could be observed in F2. Furthermore, in all three media (gangue, sediment, and soil), significant negative correlations of the percentages between F3 and F4 were observed (Fig. 3a–c). In all three media, from gangue via sediment to soil, the dominant fraction changed from F4 to F3 (Fig. 3d). Due to the dominant role of F3 + F4 (74.9 to 92.6%) in all three media, it could be assumed that the nitric acid-extractable fraction Hg (F4) can be transformed into the humic acid fraction Hg (F3) during the transportation.

As shown in Fig. S2, the dominant minerals of quartz, anatase, kaolinite, and montmorillonite were observed in gangue, sediment, and paddy soil, suggesting that sediment

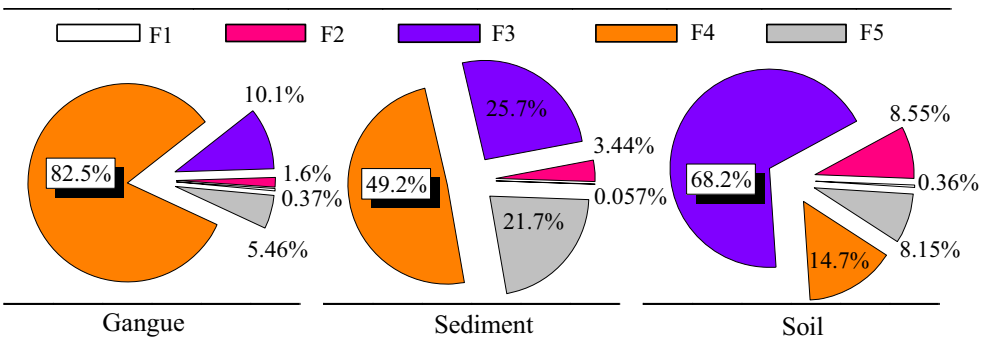

Fig. 2 Percentages of Hg speciation in gangue, sediment, and soil

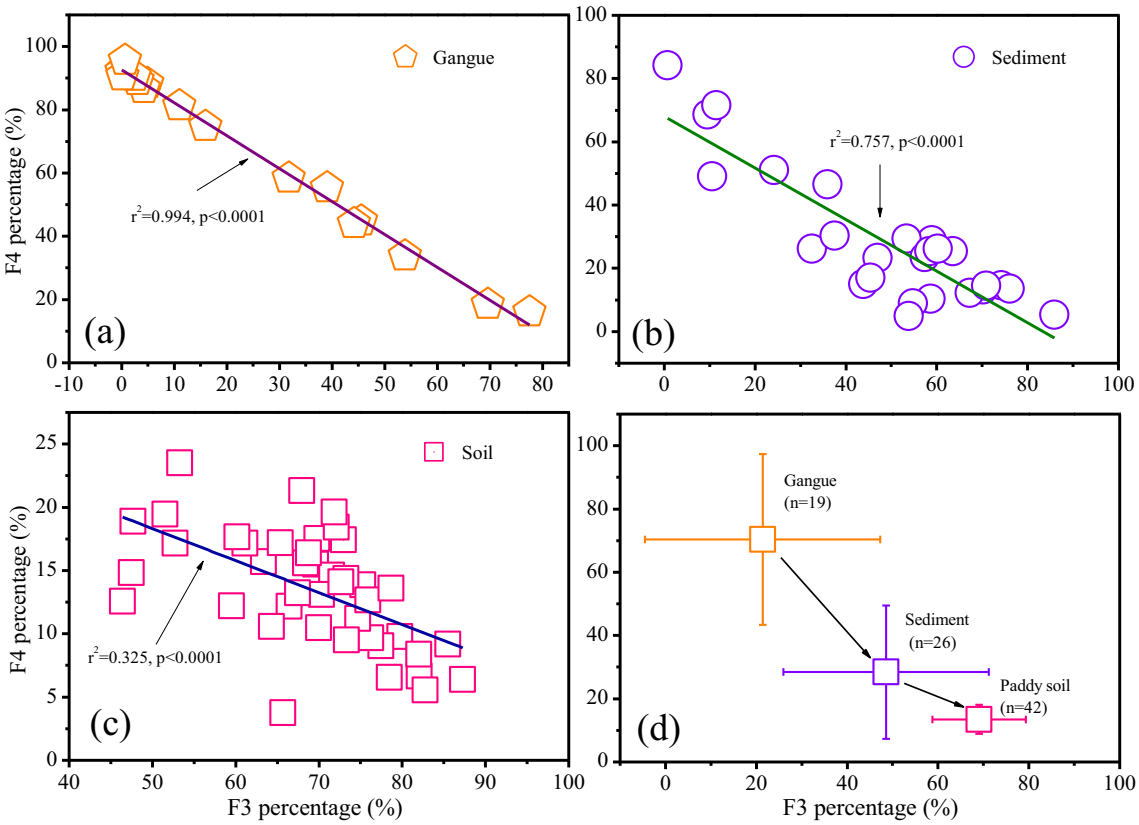

Fig. 3 Plot of correlations between F3 and F4 in gangue, sediment, and soil

and soil were impacted by the gangue. In contrast, pyrite rather than jarosite was observed in both the sediment and soil samples. Both jarosite and pyrite are considered as potential sources of acid generation in aquatic systems (Liu et al. 2018). The decomposition of jarosite in gangue can easily release sulfate and hydrogen ions, producing acidic conditions in the surroundings (Bigham and Nordstrom 2000). In return, the acidic conditions would strengthen the desorption of Hg from the solid into the aqueous phase (Geen et al. 1991; Nelson and Lamothe 1993).

The roles of organic matter, humic acid, and fulvic acid under acidic conditions on Hg biogeochemistry across coal mining areas

Gangue, sediment, and soil samples usually contain the sulfur-bearing minerals jarosite and pyrite, resulting in sulfuric acid and strongly acidic environmental surroundings (Javier et al. 2005). The surface water, flowing through coal mining areas, exhibited strong acidity, with the pH ranging from 2.0 to 5.1. In addition, both sediments and paddy soils exhibited low pH values with averages of 4.3 (range 2.2–7.2) and 5.9 (range 4.3–7.1), respectively. The concentrations of THg in sediment and soil negatively correlated with the pH values ($r^2 = 0.409$, $p < 0.001$; Fig. 4a). The correlation between the THg and pH suggests that significant amounts of Hg might be released from gangue under certain acidic conditions (Manceau et al. 2018). Moreover, the acidic conditions can heavily increase the mobility and transformation of Hg as well as the organic matter in the environment (Fernández-Martínez et al. 2015). Thus, once the water is used for irrigation, soils may be contaminated by Hg.

Significant positive correlations between THg and TOC ($r^2 = 0.271$, $p < 0.005$) as well as between THg and n-HAs ($r^2 = 0.328$, $p < 0.0001$) were observed, confirming their controlling role for THg in both sediment and soil (Fig. 4b, c). Significant positive correlations between THg and TOC ($r^2 = 0.438$, $p < 0.001$), THg and n-HAs ($r^2 = 0.268$, $p < 0.05$) in soil were observed (Fig. S3). Similarly, THg had significant positive correlations with TOC ($r^2 = 0.278$, $p < 0.01$) and n-HAs ($r^2 = 0.416$, $p < 0.01$) in sediment (Fig. S4). However, in Fig. 4b and c, highest THg value points can be found, which is highly biased, once omitting this point, higher r^2 values (0.429 in Fig. 4b, 0.546 in Fig. 4c) can be obtained, suggesting the weights of the point are 15.8% and 21.8% in Fig. 4b and c, respectively. And the highest values in both Fig. 4b and c were collected at X02 nearby the gangue piles, which implied the impact of gangue piles and indicated that gangue piles could act as the primary Hg sources to the local environment. No correlation was observed between MeHg and HAs; however, a significant correlation between the FAs and MeHg ($r^2 = 0.185$, $p = 0.0037$) (Fig. 4d) was found. Those phenomena indicate that a high TOC, particularly n-HAs in soils, can bind more Hg under certain acidic conditions

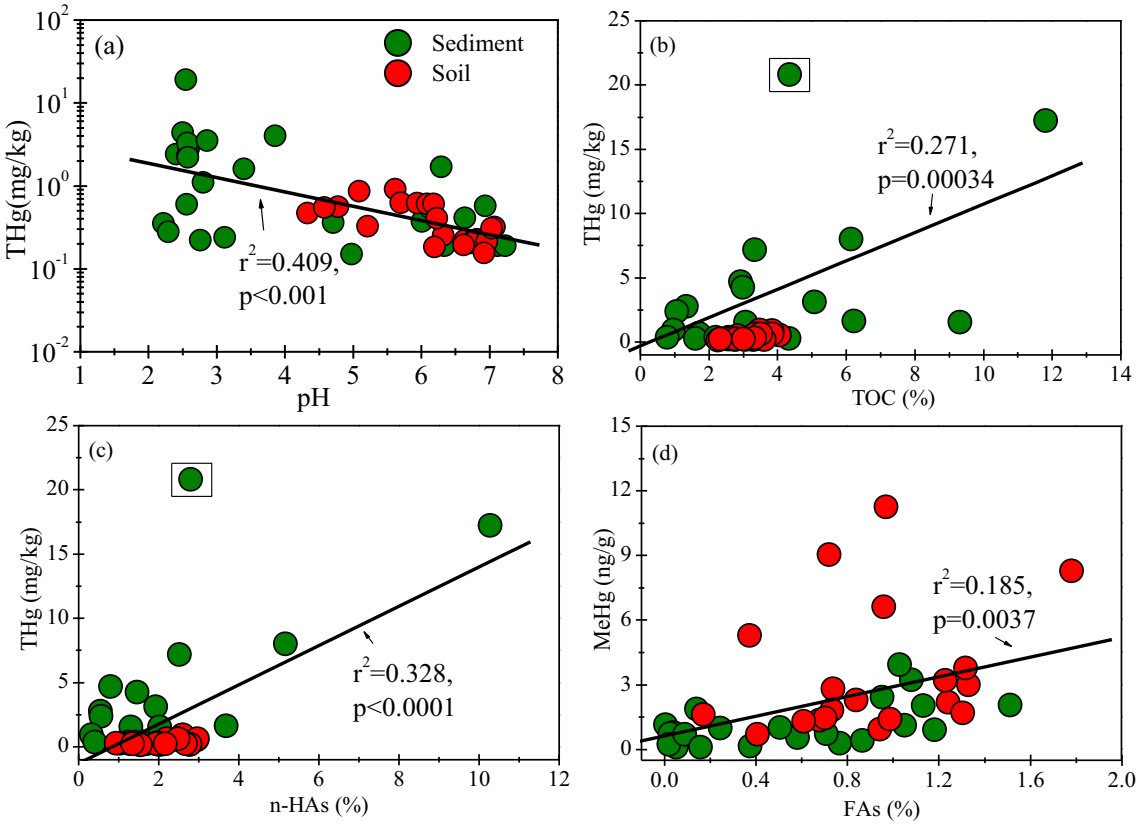

Fig. 4 Plots correlations between pH, TOC, n-HAs, and THg in sediment and soil; FAs and MeHg in sediment and soil

(Bäckström et al. 2003). The phenomena that MeHg shows a significant correlation with FAs in acidic conditions, HAs in alkaline conditions may be explained by the properties of HAs and FAs. It is well known that HAs and FAs are pH dependent, and HAs is soluble in alkaline conditions rather than acidic conditions (Sparks et al. 1996). In contrast, FAs are soluble in water under all pH conditions and can still remain in solution after the removal of the HAs by acidification (Uwayezu et al. 2019). Thus, in this study, under acidic conditions, HAs bound with Hg will deposit in the stable state; nevertheless, FAs bound with Hg in the soluble state, which are more bioavailable than HAs bound with Hg. This could explain the significant positive correlation between FAs and MeHg as well as the significant positive correlation between n-HAs and THg observed in the present study.

Rice THg and MeHg were positively correlated with the soil TOC ($r^2 = 0.260$, $p = 0.023$; $r^2 = 0.348$, $p = 0.0059$; Fig. 5a). Similarly, rice THg and MeHg show positively

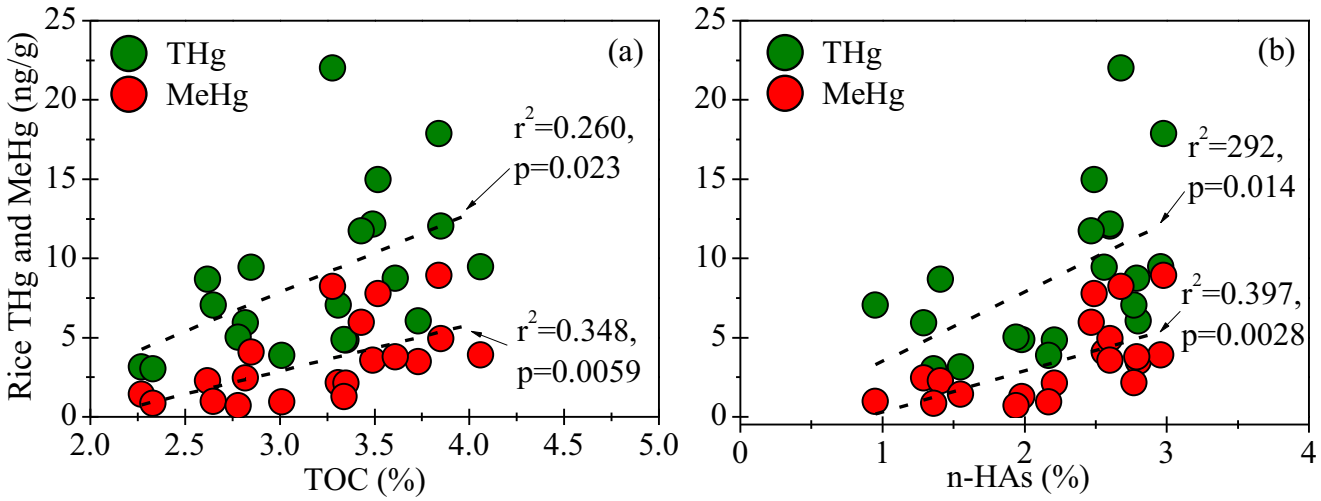

Fig. 5 Plots of correlations between soil TOC, n-HAs and rice THg, and MeHg

correlation with soil n-HAs ($r^2 = 0.292$, $p = 0.014$; $r^2 = 0.397$, $p = 0.0028$; Fig. 5b). These phenomena probably indicate that THg and MeHg binding to soil n-HAs are bioavailable and can be taken up by rice. In comparison with n-HAs, under acidic conditions, once Hg or MeHg are absorbed onto soil HAs, which become stable and are unbioavailable for rice plant (Bäckström et al. 2003; Xu et al. 2019). However, under alkaline conditions, both FAs and HAs are generally positively correlated with the Hg in rice ($r^2 = 0.372$, $p < 0.001$) (Qiu et al. 2012b). Thus, it may be concluded that low pH decreases the solubility of humic acid and then decreases of soluble organic matter, resulting in low bioavailability of Hg. Correspondingly, this will cause the similar change of Hg in rice grain.

Conclusions

This study revealed the contamination and mobility of Hg in gangue, water, sediment, and soil impacted by coal mining activities, and it also found elevated THg and MeHg concentrations in rice. High THg concentrations in sediments and soils were mainly a result of flooding and/or weathering of the abandoned gangue, which represents the major source of Hg in the area. The dominant Hg fractions in gangue were the nitric acid-extractable fraction (F4), which showed a significantly negative correlation with potassium hydroxide-extractable fraction (F3), indicating the potential ability of the transformation between each other under certain acidic conditions. Positive correlations of soil n-HAs with THg and sediment, soil, and rice were observed, probably due to acidic conditions and the specific roles of organic matters. Significant Hg release from gangue occurs and can cause elevated concentrations of both THg and MeHg in rice; thus, gangue must be appropriately treated. We suggest that Hg in coal and gangue is readily released and mobilized under acidic conditions, enhancing the bioavailability and methylation of Hg in coal mining areas, causing MeHg bioaccumulation in the food web. High MeHg concentrations as well as its high percentages in environmental compartments indicate that areas impacted by coal mining activities are Hg-sensitive ecosystems. In the future, a more comprehensive study should be conducted to reveal the fate and transformation of Hg under certain acidic conditions around other coal mining areas.

Acknowledgment The authors would like to acknowledge and appreciate Dr. Yong Meng who conducted the XRD analysis.

Funding information This research was financially supported by the Chinese National Science Foundation-Guizhou Provincial People's Government Karst Science Research Center project, Environmental Pollution Processes of Heavy Metals in Karst Terrain and Control Mechanism (No. U1612442), and Chinese National Science Foundation (No. 41463008).

References

AMAP/UNEP (2013) AMAP/UNEP geospatially distributed mercury emissions dataset 2010v1. Available at: http://www.amap.no/mercury-emissions/datasets. Accessed 4 Nov 2015

Bäckström M, Dario M, Karlsson S, Allard B (2003) Effects of a fulvic acid on the adsorption of mercury and cadmium on goethite. Sci Total Environ 304:257–268

Bai XF, Li WH, Chen YF, Yang Y (2007) The general distributions of trace elements in Chinese coals. Coal Qual Technol 1:1–4 (in Chinese with English abstract)

Bigham JM, Nordstrom DK (2000) Iron and aluminum hydroxysulfates from acid sulfate waters. Rev Mineral Geochem 40:351–403

Bloom NS, Preus E, Katon J, Hiltner M (2003) Selective extractions to assess the biogeochemically relevant fractionation of inorganic mercury in sediments and soils. Anal Chim Acta 479:233–248

BP: BP Statistical Review of World Energy (2015) Available at: http://www.biee.org/meeting-list/bp-statistical-review-worldenergy-2015. Accessed 10 June 2015

Cai F, Liu ZG, Lin BQ, Li W, Lu Z (2008) Study on trace elements in gangue in Huainan mining area. J China Coal Soc 33:892–897 (in Chinese with English abstract)

Cui LP, Bai JF, Huang WH, Shi YH, Yan SL, Tang XY, Hu YB, Xiong Y (2004) Environmental trace elements in coal mining wastes in Huainan coalfield. Geochimica 33:535–540 (in Chinese with English abstract)

Dai SF, Zeng RS, Sun YZ (2006) Enrichment of arsenic, antimony, mercury, and thallium in a Late Permian anthracite from Xingren, Guizhou, Southwest China. Int J Coal Geol 66:217–226

Dai SF, Ren D, Chou CL, Finkelman RB, Seredin VV, Zhou YP (2012) Geochemistry of trace elements in Chinese coals: a review of abundances, genetic types, impacts on human health, and industrial utilization. Int J Coal Geol 94:3–21

Determination of the composition of soil humus (2010) Sodium pyrophosphate-sodium hydroxide extraction of potassium dichromate oxidizing capacity method (NY-T-1867-2010, in Chinese) (In Chinese)

Fernández-Martínez R, Larios R, Gómez-Pinilla I, Gómez-Mancebo B, López-Andrés S, Loredo J, Ordóñez A, Rucandio I (2015) Mercury accumulation and speciation in plants and soils from abandoned cinnabar mines. Geoderma 253-254:30–38

Galloway ME, Branfireun BA (2004) Mercury dynamics of a temperate forested wetland. Sci Total Environ 325:239–254

GB 2762–2012 (2012) National Safety Standard for Food and Maximum Levels of Contaminants in Foods. Ministry of Health of the People's Republic of China

Geen VA, Boyle EA, Moore WS (1991) Trace metal enrichments in waters of the Gulf of Cadiz, Spain. Geochim Cosmochim Acta 55:2173–2191

Hintelmann H, Harris R, Heyes A, Hurley JP, Kelly CA, Krabbenhoft DP, Lindberg S, Rudd JWM, Scott KJ, Louis VLS (2002) Reactivity and mobility of new and old mercury deposition in a boreal forest ecosystem during the first year of the Metaalicus study. Environ Sci Technol 36(23):5034–5040

Hua CY, Zhou GZ, Yin X, Wang CZ, Chi BR, Cao YY, Wang Y, Zheng Y, Cheng ZR, Li RY (2018) Assessment of heavy metal in coal gangue: distribution, leaching characteristic and potential ecological risk. Environ Sci Pollut Res 25:32321–32331

Javier SE, Enrique LP, Santofimia E, Aduvire O, Jesús R, Barettino D (2005) Acid mine drainage in the Iberian Pyrite Belt (Odiel river watershed, Huelva, SW Spain): geochemistry, mineralogy and environmental implications. Appl Geochem 20:1320–1356

Ketris MP, Yudovich YE (2009) Estimations of Clarkes for Carbonaceous biolithes: world averages for trace element contents in black shales and coals. Int J Coal Geol 78:135–148

Korosi JB, Katherine G, Smol JP, Blais JM (2018) Trends in historical mercury deposition inferred from lake sediment cores across a climate gradient in the Canadian high arctic. Environ Pollut 241:459–467

Lee CS, Fisher NS (2017) Bioaccumulation of methylmercury in a marine copepod. Environ Toxicol Chem 5:1287–1293

Li XX, Wu P (2017) Geochemical characteristics of dissolved rare earth elements in acid mine drainage from abandoned high-As coal mining area, southwestern China. Environ Sci Pollut Res 24:20540–20555

Li R, Wu H, Ding J, Fu WM, Gan LJ, Li Y (2017) Mercury pollution in vegetables, grains and soils from areas surrounding coal-fired power plants. Sci Rep 7:1–9

Liang L, Horvat M, Cernichiari E, Gelein B, Balogh S (1996) Simple solvent extraction technique for elimination of matrix interferences in the determination of methylmercury in environmental and biological samples by ethylation-gas chromatography-cold vapor atomic fluorescence spectrometry. Talanta 43:1883–1888

Liang YC, Liang HD, Zhu SQ (2014) Mercury emission from coal seam fire at Wuda, Inner Mongolia, China. Atmos Environ 83:176–184

Liang YC, Liang HD, Zhu SQ (2016) Mercury emission from spontaneously ignited coal gangue hill in Wuda coalfield, Inner Mongolia, China. Fuel 182:525–530

Liang YC, Zhu SQ, Liang HD (2018) Mercury enrichment in coal fire sponge in Wuda coalfield, Inner Mongolia of China. Int J Coal Geol 192:51–55

Lindberg SE, Stratton WJ (1998) Atmospheric mercury speciation: concentration and behavior of reactive gaseous mercury in ambient air. Environ Sci Technol 32:49–57

Liu QY, Chen BH, Haderlein S, Gopalakrishnan G, Zhou YZ (2018) Characteristics and environmental response of secondary minerals in AMD from Dabaoshan Mine, South China. Ecotoxicol Environ Saf 155:50–58

MacDonald DD, Ingersoll CC, Berger TA (2000) Development and evaluation of consensus-based sediment quality guidelines for freshwater ecosystems. Arch Environ Contam Toxicol 39:20–31

Manceau A, Merkulova M, Murdzek M, Batanova V, Baran R, Glatze P, Saikia BK, Paktunc D, Lefticariu L (2018) Chemical forms of mercury in pyrite: implications for predicting mercury releases in acid mine drainage settings. Environ Sci Technol 52:10286–10296

Meng B, Feng XB, Qiu GL, Cai Y, Wang DY, Li P, Shang LH, Sommar J (2010) Distribution patterns of inorganic mercury and methylmercury in tissues of rice (*Oryza sativa L.*) plants and possible bioaccumulation pathways. J Agric Food Chem 58:4951–4958

Nelson CH, Lamothe PJ (1993) Heavy metal anomalies in the Tinto and Odiel River and estuary system, Spain. Estuaries 16:496–511

NSA (1994) National Standard Agency of China, tolerance limit of mercury in foods. GB 2762-94:171–173

Qiu GL, Feng XB, Wang SF, Shang LH (2005) Mercury and methylmercury in riparian soil, sediments, mine-waste calcines, and moss from abandoned Hg mines in east Guizhou province, southwestern China. Appl Geochem 20:627–638

Qiu GL, Feng XB, Li P, Wang SF, Li GH, Shang LH, Fu XW (2008) Methylmercury accumulation in rice (*Oryza sativa* L) grown at abandoned mercury mines in Guizhou, China. J Agric Food Chem 56:2465–2468

Qiu GL, Feng XB, Meng B, Sommar J, Gu CH (2012a) Environmental geochemistry of an active Hg mine in Xunyang, Shaanxi Province, China. Appl Geochem 27:2280–2288

Qiu GL, Feng XB, Meng B, Wang X (2012b) Methylmercury in rice (*Oryza sativa* L.) grown from the Xunyang Hg mining area, Shaanxi Province, northwestern China. Pure Appl Chem 84:281–289

Querol X, Izquierdo M, Monfort E, Alvarez E, Font O, Moreno T, Alastuey A, Zhuang X, Lu W, Wang Y (2008) Environmental characterization of burnt coal gangue banks at Yangquan, Shanxi Province, China. Int J Coal Geol 75:93–104

Ren DY, Zhao FH, Dai SF, Zhang JY, Luo KL (2006) Geochemistry of trace elements in coals. Science Press, Beijing

Shipp WG, Zierenberg RA (2008) Pathways of acid mine drainage to clear lake: implications for mercury cycling. Ecol Appl 18:A29–A54

Sparks DL, Page AL, Helmke PA, Loeppert RH, Soltanpour PN, Tabatabai MA, Johnston CT, Sumner ME (1996) Methods of soil analysis. In: Part 3 - Chemical Methods

Tian HZ, Lu L, Hao JM, Gao JJ, Cheng K, Liu KY, Qiu PP, Zhu CY (2013) A review of key hazardous trace elements in Chinese coals: abundance, occurrence, behavior during coal combustion and their environmental impacts. Energy Fuel 27:601–614

Ullrich SM, Tanton TW, Abdrashitova SA (2001) Mercury in the aquatic environment: a review of factors affecting methylation. Crit Rev Environ Sci Technol 31:241–293

UNEP (2018) Global Mercury Assessment 2018. UN Environment Programme, Chemicals and Health Branch Geneva, Switzerland

USEPA (1999) Method 1631, Revision B: Mercury in water by Oxidation, Purge and Trap, and Cold Vapor Atomic Fluorescence Spectrometry. United States Environmental Protection Agency, pp 1–33

USEPA (2001) Method 1630: Methyl mercury in water by distillation, aqueous ethylation, purge and trap, and CVAFS. Draft January 2001. U.S. Environmental Protection Agency, Office of Water, Office of Science and Technology Engineering and Analysis Division (4303), 1200 Pennsylvania Avenue NW, Washington, D.C. 20460, pp 1–41

USEPA (2002) Method 1631 E: Mercury in Water by Oxidation, Purge and Trap, and Cold Vapor Atomic Fluorescence Spectrometry. U.S. Environmental Protection Agency. EPA 821-R-02-019

Uwayezu JN, Yeung LWY, Bäckström M (2019) Sorption of PFOS isomers on goethite as a function of pH, dissolved organic matter (humic and fulvic acid) and sulfate. Chemosphere 233:896–904

Wang SX, Zhang L, Zhao B, Meng Y, Hao JM (2012) Mitigation potential of mercury emissions from coal-fired power plants in China. Energy Fuel 26:4635–4642

Wang DB, He DD, Liu XR, Xu QX, Yang Q, Li XM, Liu YW, Wang QL, Ni BJ, Li HL (2019) The underlying mechanism of calcium peroxide pretreatment enhancing methane production from anaerobic digestion of waste activated sludge. Water Res 164:1–11

Wu P, Tang CY, Liu CQ, Zhu LJ, Pei TQ, Feng LJ (2009) Geochemical distribution and removal of As, Fe, Mn and Al in a surface water system affected by acid mine drainage at a coalfield in Southwestern China. Environ Geol 57:1457–1467

Wu QR, Wang SX, Liu KY, Li GL, Hao JM (2018) Emission-limit-oriented strategy to control atmospheric mercury emissions in coal-fired power plants towards the implementation of the Minamata Convention. Environ Sci Technol 52:11087–11093

Wu YG, Yu XY, Hu SY, Shao H, Liao Q, Fan YR (2019) Experimental study of the effects of stacking modes on the spontaneous combustion of coal gangue. Proc Saf Environ 123:39–47

Xu XH, Meng B, Zhang C, Feng XB, Gu CH, Guo JY, Biahop K, Xu ZD, Zhang SS, Qiu GL (2017a) The local impact of a coal-fired power plant on inorganic mercury and methyl-mercury distribution in rice (Oryza sativa L.). Environ Pollut 223:11–18

Xu XH, Lin Y, Meng B, Feng XB, Xu ZD, Jiang YP, Zhong WL, Hu HY, Qiu GL (2017b) The impact of an abandoned mercury mine on the environment in the Xiushan region, Chongqing, southwestern China. Appl Geochem 88:267–275

Xu XH, Yan M, Liang LC, Lu QH, Han JL, Liu L, Feng XB, Wang YJ, Qiu GL (2019) Impacts of selenium supplementation on soil mercury speciation, and inorganic mercury and methylmercury uptake in rice (Oryza sativa L). Environ Pollut 249:647–654

Zhai JD, Guo SQ, Wei XX, Cao YZ, Gao LB (2015) Characterization of the modes of occurrence of mercury and their thermal stability in coal gangues. Energy Fuel 29:8239–8245

Zhang JY, Ren DY, Zheng CG, Zeng RS, Chou CL, Liu J (2002) Trace element abundances in major minerals of Late Permian coals from southwestern Guizhou province, China. Int J Coal Geol 53:55–64

Zhang CP, Wu P, Tang CY, Tao XZ, Han ZW, Sun J, Liu H (2013) The study of soil acidification of paddy field influenced by acid mine drainage. Environ Earth Sci 70:2931–2940

Zhang L, Wang SX, Wang L, Wu Y, Duan L, Wu QR, Wang FY, Yang M, Yang H, Hao JM, Liu X (2015) Updated emission inventories for speciated atmospheric mercury from anthropogenic sources in China. Environ Sci Technol 49:3185–3194

Zhao YC, Zhang JY, Chou CL, Li Y, Wang ZH, Ge YT, Zheng CG (2008) Trace element emissions from spontaneous combustion of gob piles in coal mines, Shanxi, China. Int J Coal Geol 73:52–62

Zhao YC, Yang JP, Ma SM, Zhang SB, Liu H, Gong BG, Zhang JY, Zheng CG (2017) Emission controls of mercury and other trace elements during coal combustion in China: a review. Int Geol Rev 60:1–33